Clean Energy Transportation Services: A Life-Cycle Cost Framework

Stephen Comello
Stanford Graduate School of Business
scomello@stanford.edu

Gunther Glenk
School of Business, University of Mannheim
glenk@uni-mannheim.de

Stefan Reichelstein
School of Business, University of Mannheim,
Stanford Graduate School of Business
reichelstein@uni-mannheim.de

May 2020

Abstract

The rapid deployment of electric vehicles is widely viewed as a promising path towards decarbonizing the transportation sector. The pace at which electric vehicles will replace those with internal combustion engines will depend to a large extent on cost. We present and analyze a generic life-cycle cost model in which operating costs are presumed to be driven by hours of operation. Our model framework yields critical utilization rates for ranking multiple drivetrains in terms of cost. The critical utilization rate is also shown to be the relevant criterion for optimally configuring a mix of multiple drivetrains within a fleet. We calibrate our model framework in the context of an urban transit buses system and examine how the cost comparison between diesel and battery-electric buses depends on the specifics of the duty cycle (route). Our findings suggest that even under less favorable duty cycles, battery-electric buses will entail lower life-cycle costs once utilization rates exceed approximately 20%.

Keywords: transportation services, electric vehicles, life-cycle cost, fleet cost

1 Introduction

The global quest for energy decarbonization has increasingly focused on the transportation sector[1–3]. The impending climate crisis, in combination with concerns about local air pollution, provide a growing impetus to replace internal combustion engines with zero-emission drivetrains[4;5]. In the context of passenger road vehicles, the recent advances in mobility-as-a-service also suggest that the traditional ownership model will increasingly be replaced by fleet ownership[6–8]. End-users will then be able to meet their transportation needs through spot market service arrangements. These two trends are likely to reinforce each other on account of higher utilization rates associated with vehicle sharing and comparatively lower operating costs of clean energy vehicles[9–12]. The pace at which these transportation services will be adopted in the future hinges on cost comparisons across alternative drivetrains and the sensitivity of costs to vehicle utilization rates.

This paper adds to the extensive literature on the economics of transportation services by proposing and examining a life-cycle cost metric for transportation services. Our metric, called the Levelized Cost per X-mile (LCXM), extends earlier life-cycle cost measures and complements the familiar Total Cost of Ownership (TCO) metric[13–17]. As the name suggests, the TCO seeks to capture the total present value cost associated with a transportation vehicle[17–20]. The LCXM, in contrast, measures the life-cycle cost per unit of a transportation service, such as a ton- or passenger-mile delivered.

This paper first provides a model framework for the LCXM metric and then calibrates this metric in the context of transit buses. Our model is predicated on the notion that operating costs are "driven" by the hours of vehicle operation. The LCXM metric then yields the cut-off point in terms of annual operating hours that make one drivetrain more economical than another. Relying on cost- and operational data from Stanford University's transportation department, we specifically contrast the life-cycle cost of battery-electric buses with that of diesel buses. While the former entail a substantially higher acquisition cost, they also result in a lower life-cycle cost compared to diesel-powered buses, provided the annual utilization rate is at least around 1,300 hours, with the exact cut-off depending on the characteristics of the particular route served. As a reference point, the average annual utilization of transit buses in the U.S. amounts to 2,508 hours[21].

Transportation service providers, including Stanford University, frequently vary their service offerings during select hours of the week. Taking the weekly load profile of our empirical

setting as given, we demonstrate that the cut-off points emerging from the LCXM metric can also be used to identify the composition of the cost minimizing fleet of transit buses, specifically the extent to which electric buses provide baseload services, while diesel buses are relegated to operate during peak load hours. The use of the LCXM metric in this optimization is akin to the use of the levelized cost of energy storage concept in deriving the efficient size of battery storage to complement renewable power generation[22]. We conclude with a sensitivity analysis that highlights the dependence of our findings on key model parameters pertaining to public policy and general economic trends.

2 The Unit Cost of Transportation Services

The unit cost measure developed here is a direct analogue of the familiar *Levelized Cost of Electricity (LCOE)*. This metric serves as the relevant benchmark for comparing the cost of alternative power generation sources, such as natural gas versus solar PV. Expressed in dollars per kilowatt hour (kWh), the LCOE is conceptualized as the average unit revenue that an equity investor would require for all kilowatt hours produced to break-even on a particular investment[23]. This unit revenue must cover all operating expenses, repay the project debt, and attain an appropriate return for equity investors[24].

For a generic transportation service that carries physical objects across locations, our measure of output will generally be 'X-miles'. In the context of cargo transports, this measure frequently becomes *ton-miles*, i.e., if on average z tons of cargo are transported for y miles, the vehicle delivers $z \cdot y$ ton-miles. Similarly, in the context of passenger travel, the corresponding measure could be *passenger-miles*. For passenger cars, the appropriate measure may simply be *miles* if the focus is on transporting only the driver of the vehicle.

Our model is predicated on the assumption that the service delivered by the vehicle and the operational costs incurred are driven by the total time the vehicle is in operation. For a given T-year planning horizon, we denote by $\vec{h} \equiv (h_1, ..., h_T)$ the *usage profile* of a vehicle, where $0 \leq h_i \leq 8,760$ is the utilization in hours of operation in year i (a list of symbols and acronyms is provided in Supplementary Table 1). The number of miles traveled in year i is then given by the average velocity in miles/hour, $a(\theta)$, multiplied with h_i. Velocity depends on the *duty cycle*, θ, which reflects a multi-dimensional parameter capturing the relevant performance characteristics in a specific transportation context. For a transit bus, for instance, the duty cycle would include the specifics of the route including the number of

bus stops per mile, the ambient temperature, and the topography of the route.

The number of passengers or tons of cargo transported in any given year is also determined by the utilization in that year. Allowing for the possibility of a non-linear relation, we let the function $b_i(h_i|\theta)$ represent the average number of passengers or tons transported if the vehicle travels $a(\theta) \cdot h_i$ miles in year i. The total number of X-miles then becomes:

$$X_i(h_i|\theta) = b_i(h_i|\theta) \cdot a(\theta) \cdot h_i.$$

Turning to cost components, let v denote the initial acquisition expenditure for the vehicle. At the end of its useful life, the vehicle may yield a salvage value $\lambda \cdot v$, with $0 < \lambda < 1$. In terms of annual operating costs, we distinguish between variable and fixed costs in year i. The variable component, $w_i(h_i|\theta)$, varies with the hours of operation in year i. Fixed costs, $F_i(\theta)$, are by definition usage-independent. Applicable examples for variable operating costs include fuel, spare parts, and the prorated salary for the driver. In contrast, insurance, registration, and certain maintenance activities reflect fixed costs.

Aggregation of the different cost components into a single unit cost number requires a "levelization" factor given by the discounted number of X-miles that the vehicle travels over its useful life. Let r denote the applicable cost of capital that investors require for a project, with $\gamma = \frac{1}{1+r}$ denoting the corresponding discount factor. We then define the levelization factor in terms of discounted future X-miles as:

$$Y(\vec{h}|\theta) = \sum_{i=1}^{T} X_i(h_i|\theta) \cdot \gamma^i.$$

A final cost category stems from corporate income taxes and a depreciation tax shield that a firm or individual may be subject to. As shown in *Methods*, this cost category can be summarized, including the potential salvage value, in a factor Δ that adjusts the acquisition cost of the vehicle. Overall, the levelized cost per X-mile is then defined as the sum of three components:

$$LCXM(\vec{h}|\theta) = w(\vec{h}|\theta) + f(\vec{h}|\theta) + c(\vec{h}|\theta) \cdot \Delta, \tag{1}$$

where:

$$c(\vec{h}|\theta) \equiv \frac{v}{Y(\vec{h}|\theta)}, \qquad w(\vec{h}|\theta) \equiv \frac{\sum_{i=1}^{T} w_i(h_i|\theta) \cdot \gamma^i}{Y(\vec{h}|\theta)}, \qquad f(\vec{h}|\theta) \equiv \frac{\sum_{i=1}^{T} F_i \cdot \gamma^i}{Y(\vec{h}|\theta)}. \tag{2}$$

The following claim, formally established in *Methods*, states that the LCXM does satisfy our break-even criterion that investment in a vehicle has a zero net-present value if the revenue per X-mile delivered is equal to the LCXM.

Observation 1. *For a given duty cycle θ and usage profile $\vec{h}$, the $LCXM(\vec{h}|\theta)$ in* (1) *is the break-even price per X-mile.*

In comparing the LCXM of alternative drivetrains, drivetrain 2 is said to exhibit higher *marginal operating costs* (i.e., $w(\cdot)$ has a larger derivative) than drivetrain 1 if $w'_{2,i}(\cdot|\theta) > w'_{1,i}(\cdot|\theta)$ for all i and h_i. The following finding also restricts attention to the domain of *stationary usage profiles*, which satisfy $h_i = h$ for all i.

Observation 2. *Given a duty cycle θ, suppose the marginal operating cost of one drivetrain uniformly exceeds that of the other. On the domain of stationary usage profiles, the levelized cost curves, $LCXM_1(\cdot|\theta)$ and $LCXM_2(\cdot|\theta)$ intersect for at most one value of h.*

In our empirical setting described in Section 4, diesel-powered vehicles have higher (marginal) operating costs and lower initial acquisition costs than battery electric vehicles. It then follows from Observation 2 that there will be a critical annual utilization factor, say h^*, such that the battery electric vehicle entails a cost advantage whenever $h_i > h^*$ for all i, while the opposite relation holds whenever $h_i < h^*$ for all i.

3 Cost-Efficient Vehicle Fleets

This section extends the preceding life-cycle cost analysis to settings where a service provider chooses a vehicle fleet composed of multiple drivetrains. Initially, we suppose that $L(t)$ represents the load profile of vehicles that are required to operate during the t-th hour of every day of the year, in each of the next T years on the same duty cycle θ. Suppose the service provider seeks to minimize the acquisition- and ongoing operating costs of two alternative drivetrains. If drivetrain 1 involves a higher acquisition cost but also lower

operating costs than drivetrain 2, the service provider will invest in drivetrain 1 only if these vehicles will be in operation for a sufficient proportion of the time, as prescribed by $L(\cdot)$. For simplicity, we now suppose that the variable cost, $w_i(\cdot)$, per hour of operation is constant and that $w_2 > w_1$. We can then refer to drivetrain 1 as 'baseload' and drivetrain 2 as the 'peaker'.

Denoting by k_u the number of vehicles of type u, we first ignore the integer constraint on vehicles. Suppose that $L(\cdot)$ can be uniformly approximated by a polynomial on the interval $[0, 24]$ (Weierstrass Theorem), such that the maximum value of $L(t)$ on $[0, 24]$ is k_+. Thus $k_1 + k_2 \geq k_+$. Finally, let $D(k)$ denote the total amount of time in $[0, 24]$ during which at least k vehicles must be in operation according to $L(\cdot)$. Formally,

$$D(k) \equiv ||\{t \in [0, 24] | L(t) \geq k\}||, \tag{3}$$

where $||\cdot||$ denotes the total length of the intervals for which $L(t) \geq k$. Since $L(\cdot)$ can be described by a polynomial, there are at most finitely many such intervals. By construction, $D(\cdot)$ is continuous and decreasing in k. Furthermore, if $L(\cdot)$ attains its maximum at a unique point in time, the function $D(\cdot)$ assumes all values between zero and 24.

Observation 3. *Consider two drivetrains whose levelized cost curves, $LCXM_1(\cdot)$ and $LCXM_2(\cdot)$, intersect at $(h^*, ..., h^*)$ with $h^* \in [0, 8760]$. Given the daily load profile $L(t)$, the cost-minimizing number of baseload drivetrains, k_1^*, is given by:*

$$365 \cdot D(k_1^*) = h^*.$$

The intuition for this result is that in order for the total cost associated with the fleet operation to be minimized, the 'marginal' baseload vehicle (drivetrain 1) must operate for exactly $\frac{h^*}{365}$ hours per day. Otherwise the total life-cycle cost could be lowered by either replacing this last vehicle by a peaker or expanding the number of baseload vehicles. Since k_1^* will generally not be an integer, the actual cost-minimizing number of baseload drivetrains will be one of the two integers adjacent to the k_1^* identified in Observation 3. As shown in *Methods*, the overall LCXM associated with the load profile $L(\cdot)$ can be expressed as a convex combination of the two candidate LCXMs.

We finally extend the framework to settings where each day has its own distinct load profile $L_j(\cdot)$, with $1 \leq j \leq 365$. We suppose each $L_j(\cdot)$ satisfies the same technical conditions as

$L(\cdot)$ and denote by $D_j(\cdot)$ the analogue of the function $D(\cdot)$ in (3) corresponding to $L_j(\cdot)$.

Observation 4. *Under the conditions of Observation 3, suppose the daily load profiles are given by $L_j(\cdot)$. The cost-minimizing number of baseload drivetrains, k_1^*, is then given by:*

$$\sum_{j=1}^{365} D_j(k_1^*) = h^*.$$

In concluding this section, it will be instructive to relate the Total Cost of Ownership (TCO) to our LCXM concept. As mentioned in the Introduction, TCO accounts for the total discounted cost of acquiring, operating, and selling a vehicle. In principle, it therefore captures the numerator in expressions (1) and (2). Our conceptualization of the life cycle cost of transportation services is in the tradition of time-driven activity based costing systems, a construct that has been applied in multiple industries, including energy systems and health care[25;26]. Our framework extends prior studies[13;15–17] in terms of output measures (X-miles), break-even criteria (critical utilization rate) and domain application (fleet optimization).

4 Diesel vs. Battery-Electric Transit Buses

We now apply the preceding framework to Stanford University's bus service known as Marguerite. Like a municipal bus service, Marguerite interconnects the university campus and the surrounding community via multiple routes, operating daily at varying levels of capacity utilization with peaks during weekday mornings and afternoons. The majority of the service is run with transit buses (see Supplementary Table 2). Beginning in 2014, the university has gradually replaced diesel-powered with battery-electric buses.

To compare the life-cycle cost of the two drivetrains, our calculations focus on the duty cycles of two distinct routes, referred to as Route A and B. They reflect opposite ends of the range of duty cycles operated by Marguerite, with the number of bus stops per mile amounting to 1.1 for Route A and 2.7 for Route B. Since topography and ambient temperature of all campus routes are virtually identical, Routes A and B generally yield corner solutions for all routes operated by Marguerite.

Our analysis relies on the records of Stanford's transportation department for recent cost and operational data (details provided in *Methods*). Table 1 shows average values for the main life-cycle cost components. The net acquisition cost represents the initial purchasing

price minus the salvage value and, for electric buses, a capital incentive of $100,000 granted by the California Air Resources Board[27]. The variable cost comprises fuel costs and variable maintenance costs but excludes the salary of drivers, which is the same across drivetrains.

Table 1: **Main cost parameters (in 2019 $US).**

	Diesel	**Electric**
Variable cost per hour (Route A)	$26.25	$2.02
Variable cost per hour (Route B)	$16.79	$4.77
Fixed cost per year	$5,054	$5,913
Net acquisition cost	$425,189	$631,300
Useful lifetime	12 years	12 years
Cost of capital	5.00%	5.00%

Considering the variable costs in Table 1, one might expect that more stops per mile (Route B) increases the variable cost of both drivetrains and especially that of diesel buses whose fuel consumption is more sensitive to frequent stops. This intuition is, however, misleading for diesel buses in the context of Marguerite. The increased fuel cost per mile of diesel buses for Route B is outweighed by a lower average velocity such that the fuel cost per hour of operation decreases. For electric buses, in contrast, this intuition is confirmed in Table 1. Moving from Route A to B, the fuel cost per hour of operation decreases, yet variable maintenance costs increase with the number of stops per mile for both drivetrains. The latter effect is dominant for electric buses.

Figure 1 depicts the levelized cost curves per passenger-mile (LCPM) for both drivetrains by route. Consistent with Observation 2, there is a unique critical utilization, h^*, beyond which electric buses entail lower life cycle cost. These values amount to 996 hours for Route A and 2,006 hours for Route B, marked by the solid vertical lines in Figure 1. The explanation for the counterintuitive finding that the critical utilization rate is larger for Route B than for Route A is given by the above observation: the variable cost per hour of diesel buses is lower for Route B, because the buses travel fewer miles per hour when there are more stops per mile. The critical utilization for the average duty cycle (number of stops per mile) of the entire Marguerite system amounts to 1,329 hours; see *Methods* for details.

The operational records of Stanford University show that Route A is almost exclusively served by electric buses, while the opposite holds for Route B. The average annual utilization factors amount to 1,434 hours and 1,453 hours, respectively. For these utilization factors, Figure 1 shows that the LCPM of electric buses is lower than that of Diesel buses on Route

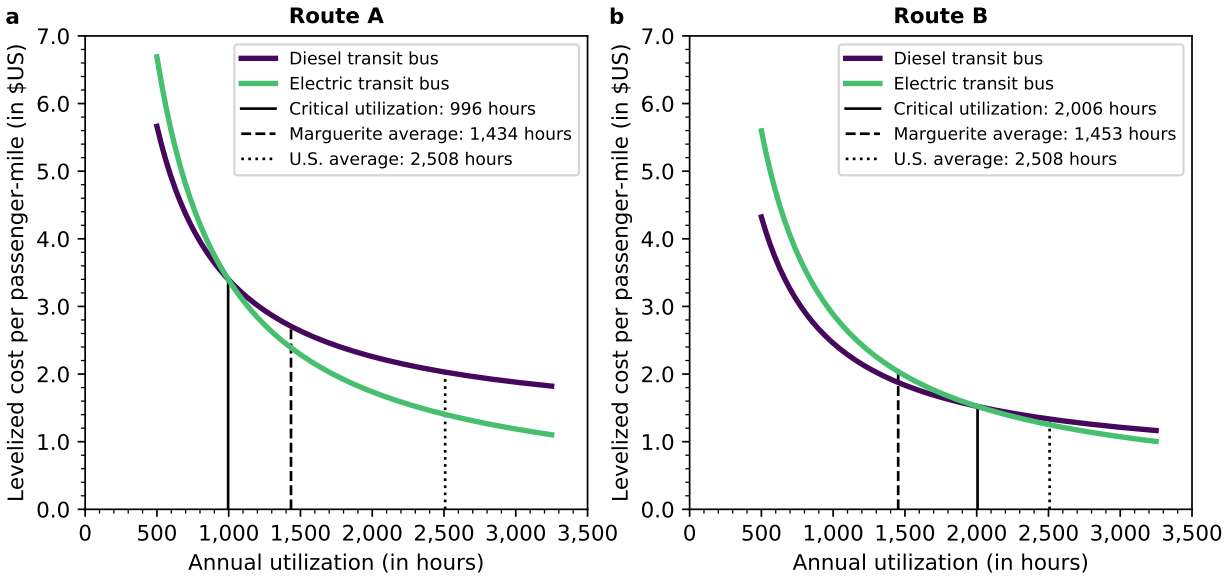


Figure 1: **Levelized cost per passenger-mile. a,b,** This figure shows the levelized cost per passenger-mile of diesel and electric transit buses for (**a**) Route A and (**b**) Route B.

A, while the opposite pattern applies on Route B. The university's reliance on these two drivetrains for the two routes thus appears consistent with the goal of minimizing the life-cycle cost of transportation services provided. For further reference, the average annual utilization of transit buses in the U.S. amounts to 2,508 hours[21]. Such high utilization rates would give electric buses a cost advantage on both routes, as shown in Figure 1.

Figure 2 depicts the daily load profiles of buses operating on the Stanford campus. If hypothetically all Marguerite buses were to run on Route A, the efficient number of diesel and electric buses would amount to 7 and 22, respectively. The corresponding values for Route B are 18 and 11. Consistent with Observation 4 and the functions $D_j(\cdot)$ being decreasing in k_1, the efficient number of electric buses for Route B is smaller than on Route A, since the corresponding critical utilization factor h^* is larger for Route B (see Figure 1).

If the number of stops per mile is taken to be the average of all routes served by Marguerite and all buses were to serve that average route, the optimal number of diesel and electric buses would be 11 and 18. For this scenario, electric buses would be operating as baseload capacity for more than the respective h^* hours per year, whereas each of the diesel buses would be operating as peakers for less than that. A general insight from our analytical framework is that it will generally be efficient to have a proper mix of baseload and peaker vehicles, unless the underlying load profile assumes an 'extreme' shape. Specifically, even if all campus routes

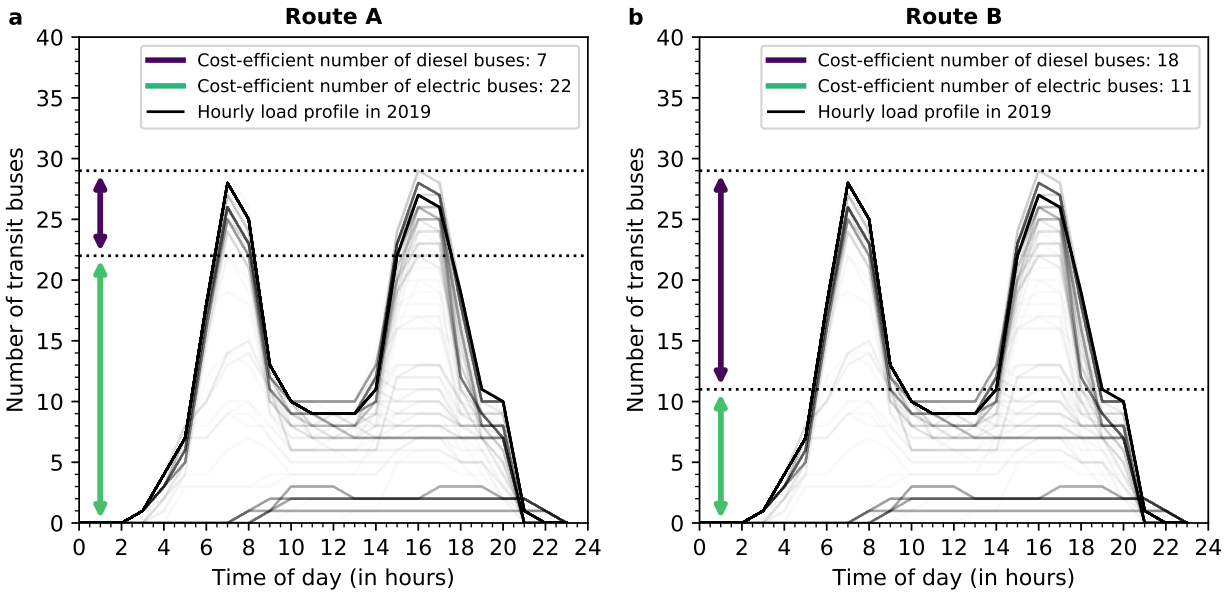


Figure 2: **Cost-efficient vehicle fleets. a,b,** This figure shows the cost-efficient number of diesel and electric transit buses for the hourly load profile of Marguerite in 2019 if hypothetically all routes exhibited a duty cycle of either (**a**) Route A or (**b**) Route B. The load profile depicted here is an overlay of the hourly profile for individual days in 2019. The more the daily profiles overlap, the darker is the shade of gray. The upper twin peaks represent load profiles on weekdays, while the lower twin peaks display the profile for weekend days.

were to correspond to the characteristics of Route B, which tends to favor Diesel buses, a planner would still want to procure 11 electric buses out of a total of 29.

Our model of fleet optimization has ignored requirements for backup capacity due to the need to accommodate irregular events on campus and the possibility of unscheduled vehicle maintenance. In fact, Stanford University currently maintains 10 transit buses over and above the annual peak demand of 29 scheduled buses. That observation is consistent with the utilization rate on both routes being significantly below the U.S. average. At the same time, given that in 2019 there were already 29 electric buses in operation, it will be advantageous for the university to reduce its reliance on diesel buses to the largest extent possible due to the lower operating costs of electric drivetrains.

5 Discussion

Since our numerical calibration of the life-cycle cost of transit buses is based on a single university service operator, it is essential to check the sensitivity of our findings to changes

in some of the key input variables. Specifically, we focus on the sensitivity of the critical utilization rate, i.e., $\frac{h^*}{8760}$, as derived in Figure 1 and the efficient share of electric buses, i.e., $\frac{k_1^*}{29}$, as derived in Figure 2. For consistency, the following comparisons focus on the same two routes in order to illustrate the impact of alternative duty cycles.

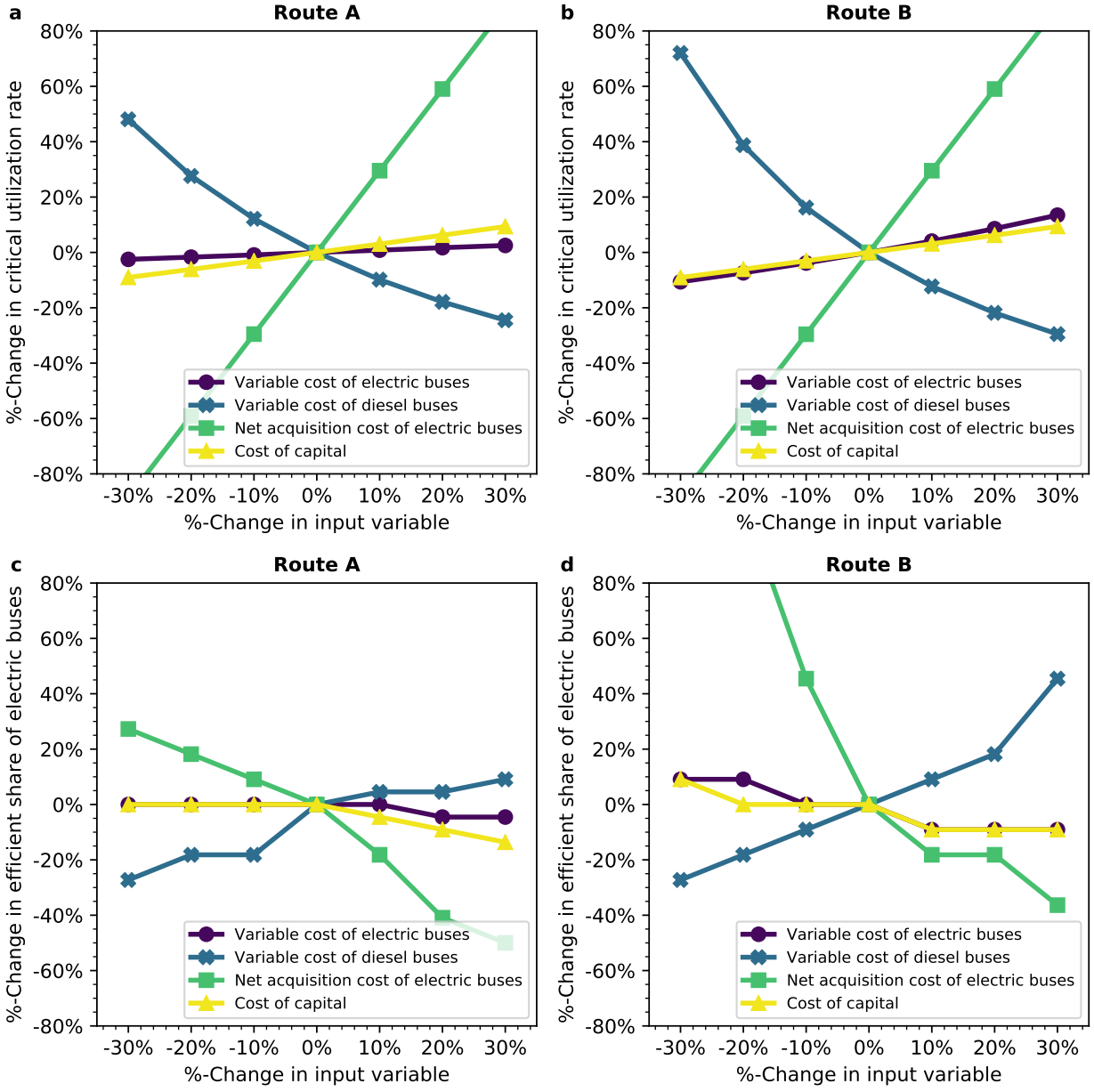


Figure 3: **Sensitivity analysis. a,b,c,d** This figure shows the sensitivity of the critical utilization rate on (**a**) Route A and (**b**) Route B, as well as the sensitivity of the efficient share of electric buses on (**c**) Route A and (**d**) Route B to four different input variables

Recent advances in lithium-ion battery technology have significantly lowered the price of

lithium-ion battery packs which, in turn, comprise a significant share of the net acquisition cost of battery electric buses. Numerous recent studies point to sustained cost reductions in the future along the trajectory of a classic learning curve[1;28;29]. An additional development that is forecast to lower the net acquisition cost of battery electric buses is the emergence of a market for "second life" battery applications[30;31], once the degradation of the battery packs makes them no longer suitable for transportation services. In the context of our model this would increase the salvage value with a corresponding decrease in the net acquisition cost of electric buses. The green lines in Figure 3 confirm that the critical utilization rate is highly sensitive to increases in the net acquisition cost of electric buses. On either route, a 10% change in the net acquisition cost results in approximately a 30% change in h^*.

Naturally, the efficient share of electric vehicles is decreasing in the net acquisition cost of electric vehicles. These decreases occur at a higher rate on Route B where the hourly operating costs of the two drivetrains are less divergent. Finally, Figures 3c and 3d indicate that without the current $100,000 capital subsidy made available to electric buses by the California Air Resource Board (CARB), the efficient share of electric vehicles in the Stanford fleet would decrease by about 25%.

The purple lines in Figure 3 indicate that both our two dependent variables are relatively insensitive to changes in the variable cost of electric buses. This observation can be attributed to the fact that variable costs constitutes only a minor share of the overall life-cycle cost of electric buses. The hourly operating cost of diesel buses may differ substantially in other application contexts as the efficiency of diesel buses improves with the emergence of diesel-electric hybrid drivetrains. Furthermore, the cost of Diesel fuel is likely to vary over time and across geographic regions, possibly because Diesel fuel may become subject to CO_2 emission charges in some jurisdictions. The blue lines in Figure 3 show that our dependent variables are relatively sensitive to changes in the variable cost of diesel buses. To calibrate the magnitude of the improved efficiency associated with hybrid buses, we note that the average variable cost of four hybrid buses within the Marguerite fleet yields a reduction of about 10% for both routes, while these buses are comparable to traditional diesel buses in other cost and operational data. According to the blue lines in Figure 3, the critical utilization rate would increase by about 15% for both routes. The corresponding impact on the efficient share of electric buses would be a decrease of also about 15%.

One would expect any increases in the cost of capital to weaken the relative competitive

position of electric buses, that is h^* to increase and k_1^* to decrease. While the LCPM of both drivetrains will increase, a larger cost of capital should have a more pronounced effect on the more capital intensive drivetrain, i.e., electric vehicles. The yellow lines in Figure 3 confirm this intuition, though the changes in the dependent variables turn out to be relatively minor for both variables and on both routes. Specifically, the critical utilization rate increases almost linearly at the modest rate of 3% for every 10% increase in the cost of capital.

Our analysis has excluded the compensation paid to drivers in order to highlight the differences in life-cycle cost between the two competing drivetrains. Inclusion of the drivers' salaries would increase the levelized cost per passenger-mile for both drivetrains at the critical utilization rate h^* by about 90% on Route A, and by about 160% on Route B. At the same time, inclusion of the drivers' compensation reduces any cost difference between electric buses and diesel buses by on average about 60% for the range of critical utilization rates shown in Figure 1. This observation could make electric buses preferable if, beyond life-cycle cost, tailpipe emissions become a choice criterion.

6 Concluding Remarks

This paper presents a life-cycle cost metric that captures the unit cost of a generic transportation service. Conceptualized as a break-even value, our time-driven variant of the LCXM metric identifies the critical utilization rate that ranks alternative drivetrains in terms of their life-cycle cost. This critical utilization rate is furthermore shown to provide the decision criterion for the cost efficient mix of alternative drivetrains in a vehicle fleet. We calibrate this metric in the context of Stanford University's bus service as a case in point. Contrasting the life-cycle cost of diesel and battery-electric buses, we find that on average electric buses have a lower LCXM if the annual utilization rate is at least around 15%. The cost minimizing fleet composition is shown to be highly dependent on the duty cycles that the transportation service seeks to cover.

Moving further afield on transit buses, it will be instructive to consider a broader array of bus types within a fleet, differentiated by duty cycle, vehicle passenger capacities, and drivetrain (e.g. a hydrogen fuel cell[32]). Alternative vehicle types could include autonomous last-mile personal mobility options that require substantially higher upfront capital expenditures in exchange for lower operating costs which no longer include the salaries of drivers. Beyond passengers, our LCXM metric is applicable to the freight domain. Current demon-

strations of cargo truck platooning show promise in increasing the utilization of transport trucks while decreasing their operational costs as do experiments with delivery drones.

7 Methods

Economic Model. We first complete the description of the model and then validate the formal claims in the main text. The tax factor, Δ, depends on both the applicable income tax rate, denoted by α, as well as the allowable depreciation schedule for tax purposes. That schedule is denoted by $\{d_t\}_{t=1}^{T}$, such that $d_t \geq 0$ and $\sum_t d_t = 1$, and determines how the initial investment is amortized for tax purposes over time. The overall effect of income taxes can be summarized by:

$$\Delta = \frac{1 - \alpha \cdot \left[\sum_{t=0}^{T} d_t \cdot \gamma^t \right]}{1 - \alpha} - \lambda \cdot \gamma^T. \tag{4}$$

If $\alpha = 0$, as will be the case for a non-profit organization like Stanford University, the tax factor reduces to $\Delta = 1 - \lambda \cdot \gamma^T$.

Proof of Observation 1: Suppose every X-mile attains a revenue of p. For a given duty cycle θ and usage profile $\vec{h}$, we demonstrate that the investment breaks even whenever $p = LCXM(\vec{h}|\theta)$. In year i, the operating revenue is given by:

$$Rev_i(h_i) = X_i(h_i|\theta) \cdot p = b_i(h_i|\theta) \cdot a(\theta) \cdot h_i \cdot p.$$

The overall pre-tax cash flow in year i will be represented by CFL_i^o. It comprises operating revenues and operating costs:

$$CFL_i^o(h_i|\theta) = X_i(h_i|\theta) \cdot p - w_i(h_i|\theta) - F_i(h_i|\theta).$$

The firm's taxable income in year i is given by:

$$I_i(h_i|\theta) = X_i(h_i|\theta) \cdot p - w_i(h_i|\theta) - F_i(h_i|\theta) - v \cdot d_i.$$

The present value of all after-tax cash flows is therefore given by:

$$\sum_{i=1}^{T} [CFL_i^o(h_i|\theta) - \alpha \cdot I_i(h_i|\theta)] \cdot \gamma^i - v + (1-\alpha) \cdot \lambda \cdot v \cdot \gamma^T. \tag{5}$$

Direct substitution shows that the expression in (5) is equal to zero if and only if:

$$(1-\alpha) \sum_{i=1}^{T} CFL_i^o(h_i|\theta) \cdot \gamma^i + \alpha \cdot \sum_{i=1}^{T} v \cdot d_i \cdot \gamma^i + (1-\alpha) \cdot \lambda \cdot v \cdot \gamma^T = 0. \tag{6}$$

Dividing by $(1-\alpha)$ and recalling the definition of the tax factor, Δ, the equality in (6) reduces to:

$$\sum_{i=1}^{T} [X_i(h_i|\theta) \cdot p - w_i(h_i|\theta) - F_i(h_i|\theta)]\gamma^i = v \cdot \Delta. \tag{7}$$

By definition $Y(\vec{h}|\theta) = \sum_{i=1}^{T} X_i(h_i|\theta) \cdot \gamma^i$ and therefore (7) holds if and only if $p = LCXM(\vec{h}|\theta)$.

■

Proof of Observation 2: For notational simplicity, we write $LCXM(h|\theta)$ instead of $LCXM(h, ..., h|\theta)$ on the domain of stationary load profiles. Suppose that contrary to the claim:

$$LCXM_1(h|\theta) = LCXM_2(h|\theta)$$

and

$$LCXM_1(h + \delta h|\theta) = LCXM_2(h + \delta h|\theta),$$

for some $\delta h > 0$. Recalling the definition of the LCXM, the existence of these two crossing points would imply:

$$\sum_{i=1}^{T} [w_{2,i}(h + \delta h|\theta) - w_{1,i}(h + \delta h|\theta)] \cdot \gamma^i = \sum_{i=1}^{T} [w_{2,i}(h|\theta) - w_{1,i}(h|\theta)] \cdot \gamma^i.$$

Equivalently,

$$\sum_{i=1}^{T} \left[\int_h^{h+\delta h} [w'_{2,i}(u|\theta) - w'_{1,i}(u|\theta)] du \right] \cdot \gamma^i = 0.$$

The assumption of one drivetrain having uniformly higher marginal operating costs than the

other would then imply:

$$\int_{h}^{h+\delta h} [w'_{2,i}(u|\theta) - w'_{1,i}(u|\theta)]du = 0,$$

for all i. The last expression would again contradict that either $w'_{2,i}(u|\theta) > w'_{1,i}(u|\theta)$ for all u, or alternatively $w'_{2,i}(u|\theta) < w'_{1,i}(u|\theta)$. ■

Proof of Observation 3: Given the load profile, $L(\cdot)$, the required total annual number of operating hours becomes:

$$\hat{h} = 365 \cdot \int_{0}^{24} L(t)\, dt.$$

For any feasible fleet composition, i.e., (k_1, k_2) such that $k_2 \geq k_+ - k_1$, the fleet operator will rely to the extent possible on the drivetrain with the lower unit operating cost. Specifically, the number of daily operating hours of drivetrain 1 will be:

$$H(k_1) \equiv \int_{0}^{24} \min\{L(t), k_1\}\, dt.$$

The overall cost minimization problem then is to choose k_1 so as to minimize the break-even price p per X-mile required to cover the fleet operator's total life-cycle cost in meeting the daily load profile $L(\cdot)$. In particular, p must satisfy the inequality:

$$\begin{aligned}\sum_{i=1}^{T} p \cdot X(\hat{h}) \cdot \gamma^i \geq v_1 \cdot k_1 + v_2 \cdot (k_+ - k_2) + \sum_{i=1}^{T} \Big[& 365 \cdot (w_1 \cdot H(k_1) + w_2 \cdot (\hat{h} - H(k_1)) \\ & + F_1 \cdot k_1 + F_2 \cdot (k_+ - k_1) + \alpha \cdot I_i(\hat{h}, k_1, p) \Big] \cdot \gamma^i \\ & - \gamma^T \cdot (1 - \alpha) \cdot \lambda \cdot (v_1 \cdot k_1 + v_2 \cdot (k_+ - k_2)).\end{aligned} \tag{8}$$

Here $I_i(\hat{h}, k_1, p)$ denotes the taxable income in year i, that is:

$$\begin{aligned}I_i(\hat{h}, k_1, p) \equiv p \cdot X(\hat{h}) - 365[(w_1 \cdot H(k_1) + w_2 \cdot (\hat{h} - H(k_2))] \\ - F_1 \cdot k_1 - F_2 \cdot (k_+ - k_1) - [v_1 \cdot k_1 + v_2 \cdot (k_+ - k_1)] \cdot d_i.\end{aligned}$$

Recalling the definition of Δ and collecting terms, the above inequality reduces to:

$$p \geq \frac{1}{\sum_{i=1}^{T} X(\hat{h}) \cdot \gamma^i} \Big[v_1 \cdot \Delta \cdot k_1 + v_2 \cdot \Delta \cdot (k_+ - k_1) + \sum_{i=1}^{T} \big[365 \cdot (w_1 \cdot H(k_1) + w_2 \cdot (\hat{h} - H(k_1)) + F_1 \cdot k_1 + F_2 \cdot (k_+ - k_1) \big] \cdot \gamma^i \Big]. \tag{9}$$

To minimize p, we differentiate the right-hand side of (9) with respect to k_1, noting that

$$H'(k_1) = \int_{\{t \in [0,24] | L(t) \geq k_1\}} dt \equiv D(k_1).$$

This derivative is given by:

$$\frac{1}{\sum_{i=1}^{T} X(\hat{h}) \cdot \gamma^i} \Big[v_1 \cdot \Delta + \sum_{i=1}^{T} [w_1 \cdot 365 \cdot D(k_1) + F_1] \cdot \gamma^i - v_2 \cdot \Delta - \sum_{i=1}^{T} [w_2 \cdot 365 \cdot D(k_1) + F_2] \cdot \gamma^i \Big].$$

Recalling the definition of the LCXM, this last expression for the derivative of the right-hand side of (9) is proportional to:

$$LCXM_1(365 \cdot D(k_1)) - LCXM_2(365 \cdot D(k_1)). \tag{10}$$

For a cost minimum, k_1 must be chosen so that the derivative expression in (10) is zero, which implies $k_1 = k_1^*$, since k_1^* is such that $365 \cdot D(k_1^*) = h^*$ and $LCXM_1(h^*) = LCXM_2(h^*)$. Furthermore, since $w_2 > w_1$ and $D(\cdot)$ is decreasing in k_1, the objective function on the right hand-side of (9) is convex in k_1. Thus the value of k_1 that sets the first-order condition in (10) equal to zero yields the global cost minimum. ■

We note in passing that the levelized cost of the optimized fleet can be expressed as a convex combination of the two component LCXM, with the respective weights given by the respective operating hours of the two drivetrains. For simplicity, suppose that $b_i(h_i) = b$. Referring back to (9), it is then straightforward to verify that the LCXM of the optimized

fleet is equal to:

$$LCXM(365 \cdot \hat{h}) = \frac{365 \cdot H(k_1^*)}{\hat{h}} \cdot LCXM_1(365 \cdot H(k_1^*)) + (1 - \frac{365 \cdot H(k_1^*)}{\hat{h}}) \cdot LCXM_2(365 \cdot (\hat{h} - H(k_1^*))). \quad (11)$$

Proof of Observation 4: The proof of Observation 4 mirrors that of Observation 3. The total number of vehicles acquired now becomes k_+ given by the maximum value across all $L_j(\cdot)$. With regard to the expression in (8), the only change is that the variable operating costs now become:

$$\sum_{i=1}^{T}[w_1 \cdot \sum_{j=1}^{365} H_j(k_1) + w_2 \cdot \sum_{j=1}^{365}(\hat{h}_j - H_j(k_1))] \cdot \gamma^i,$$

where

$$\hat{h}_j = \int_0^{24} L_j(t)\, dt \;\text{ and }\; H_j(k_1) \equiv \int_0^{24} \min\{L_j(t), k_1\}\, dt.$$

The claim in Observation 4 then follows by proceeding exactly as in the proof of Observation 3. ■

Input Usage and Cost Data. The data on input usage and cost items are furnished by various information systems at Stanford University related to energy- and fleet management. Table 2 provides average values for route-invariant cost parameters for both diesel and electric buses. The acquisition cost shown there for each bus type reflects the most recent purchase price. If the purchase occurred before the year 2019, we adjusted the price for inflation with an average annual inflation rate of 2.0%. The capital incentive for electric buses is a subsidy granted by the California Air Resources Board under the Hybrid and Zero-Emission Truck and Bus Voucher Incentive Program[27]. The salvage value for each drivetrain is based on an estimate provided by Stanford. To assess fixed costs, we took the drivetrain-specific average across transit buses in the Marguerite fleet of annual operations and maintenance costs for the years 2017–2019. The annual fixed cost of each bus comprises the sum of registration fees, insurance cost, and components of maintenance costs that are usage-independent, as shown in Supplementary Note 2. The labor cost per hour includes the cost of the driver per hour of operation, composed of salary, benefits, and overhead. Our estimate of the fuel costs is based on the average of diesel prices per gallon paid by Stanford in 2019.

The cost of electricity charging for EV buses deserves particular attention. Stanford pur-

Table 2: **Route-invariant cost parameters (in 2019 $US).**

	Diesel	**Electric**
Acquisition cost	$430,757	$750,000
Capital incentive	–	$100,000
Salvage value	$10,000	$38,750
Fixed cost per year	$5,054	$5,913
Labor cost per hour	$71.00	$71.00
Fueling cost per gallon	$3.40	–
Charging cost per kWh	–	$0.092
Useful lifetime	12 years	12 years
Cost of capital	5.00%	5.00%

chases electricity from a variety of sources each entailing a specific set of fixed, demand and volumetric charges. The total of these electricity costs in 2019 normalized by the total volume of electricity delivered (kWh) amounts to $0.092/kWh, which represents the average cost of electricity to the university on a volumetric basis. This cost figure is charged to all administrative units within the university for the consumption of electricity. In addition, each unit is charged a markup for various overhead cost items, resulting in a total of $0.152/kWh[33]. For the purpose of determining the life-cycle cost of EV buses, we only impute the normalized volumetric rate, and exclude the university-wide overhead charge, as this is the effective incremental cost per kWh to the university.

A time-invariant volumetric charge for electricity seems appropriate given the configuration of Stanford's energy system. While the campus as a whole is subject to demand charges and time-of-use volumetric charges, these time-dependent costs are essentially not relevant to the various operating units, including the bus depot, due to the dominance of the university's central energy facility. The facility manages the district heating and cooling for the entire campus and is, therefore, by far the largest single source of electricity demand, dwarfing, in particular, the incremental load associated with bus charging. The central energy facility has effectively the ability to ramp the university's demand for power in response to time-based price signals, thus enabling the campus to minimize both demand and time-of-use charges[34]. We note that time-invariant volumetric charges for electric buses have also been imputed in other settings applicable to university campuses and municipal bus fleets[35;36].

The variable cost components include certain maintenance and energy costs, whereby the latter is the product of the route-specific energy consumption and the fueling or charging

rate provided in Table 2. Our dataset includes the variable maintenance costs and energy consumption per transit bus in the Marguerite fleet for the years 2017–2019 on the specific days these costs were incurred. These variable cost components vary by route depending on the number of stops per mile and the collection of routes served by a bus throughout the year. The number of buses assigned to each route was assumed to be constant across the years.

Table 3 provides average values for the variable cost for both drivetrains by route. Supplementary Note 2 shows which categories of the maintenance cost are considered to be usage-dependent for each drivetrain. For Route A, for instance, the average variable maintenance cost is calculated by taking the average across buses for which the annual average number of bus stops per mile is equal to that of Route A.

Route-specific energy consumption for electric and diesel drivetrains are calculated according to different methods which reflect differences in the availability of data. For electric buses, we rely on daily total net energy consumption, total time in service, and total distance traveled as provided by the battery management system (BMS) for individual buses. Net energy consumption in this context refers to the total energy provided to the bus from the battery minus the energy generated via regenerative braking . We gathered the three categories of the BMS data for electric transit buses that operated on Route A and B most frequently in 2019. To account for daily and seasonal variation, we attained for each bus a complete BMS record for a randomly selected day in each month between January–August 2019. This produced 24 records (3 bus readings per month for 8 months) per route. The figures shown in Table 3 for electric buses represent the route-specific average of the 24 measures. The time component of this measure accounts for the actual time a bus was servicing a route. This includes in-service idling but not mid-day lulls when the bus was not in service. As a point of reference, the energy consumption per hour presented in Table 3 corresponds to a power consumption of 1.41 kWh/mi and 1.11 kWh/mi for Routes A and B, respectively.

For diesel buses, we calculate energy consumption per bus by dividing the total volume (in gallons) dispensed during each refueling event to a specific bus by the total number of in-service hours of the bus within the time interval since the last refueling event for all refueling events recorded in 2019. The corresponding set of bus stops per mile for each bus is calculated based on the duty cycles performed during the same in-service time intervals. The figures in Table 3 result from taking the mean of the calculated per-bus energy consumption

Table 3: **Route-specific cost parameters (in 2019 $US).**

	Route A	Route B	Average
Diesel			
Variable maintenance cost per hour	$5.09	$8.37	$7.04
Energy consumption per hour (in gallons)	6.23	2.48	4.44
Fueling cost per hour	$21.16	$8.42	$15.07
Variable cost per hour	$26.25	$16.79	$22.11
Electric			
Variable maintenance cost per hour	$1.18	$4.46	$3.13
Energy consumption per hour (in kWh)	9.13	3.34	9.01
Charging cost per hour	$0.84	$0.31	$0.83
Variable cost per hour	$2.02	$4.77	$3.96

measures corresponding to those buses that exhibited stops per mile measures similar to Route A or Route B, windsorized at the 5.0% level. Since the refueling data includes the entire year 2019, the average consumption values account for variations across days, seasons, and vehicles. For reference, the energy consumption per hours given in Table 3 correspond to a fuel economy of 5.26 miles per gallon and 2.61 miles per gallon for Routes A and B, respectively. These values are relatively low because they account for fuel consumed during in-service idling and unplanned maintenance that require idling for troubleshooting.

Route Information. Route data for Marguerite was provided by Stanford. Table 3 provides the main route characteristics for Route A and B, as well as the simple average for these parameters across all routes in the system. Route data for all routes is provided in Supplementary Note 1. The number of bus stops per mile is calculated by dividing the total route distance by the number of bus stops. Finally, average velocity is determined by dividing the total route distance by the expected completion time as provided by Stanford Transportation.

Table 4: **Route A, Route B and Marguerite average data.**

	Route A	Route B	Average
Number of bus stops per mile	1.1	2.7	1.9
Average velocity (in miles per hour)	7.4	3.0	8.7
Average number of passengers	3.2	9.4	6.9
Marguerite average utilization (in hours)	1,434	1,453	1,607

In Table 3, the average number of passengers represents the number of passengers trans-

ported across the full distance of a route. This value is the average number of passengers per hour multiplied with the average passenger-miles per passenger and dividing this product by the average velocity. The number of passengers per hour, in turn, is determined by dividing the annual number of passengers that traveled a particular route by the annual total number of hours that the route was serviced. The average passenger-miles per passenger is estimated due to a lack of detailed on-boarding and off-boarding events per passenger as the expected distance in miles that the average passenger would travel on a given route. This figure is defined as the average distance between the two most popular bus stops on a route. The term popular here refers to the bus stops on a route that have the highest total number of passengers boarding over the course of a year. Given that bus routes are loops that begin and end at the same location, the average distance can be conceptualized as the average length of the two arcs that connect two points on a circle.

For the average utilization, we first calculate the operating hours of each bus in 2019 as the product of the total number of loops per route that a bus accumulated in 2019 with the expected completion time per route. Since we only have data on bus-route assignments for the year 2019, we calculate the operating hours of each bus in 2017 and 2018 by scaling the respective value for 2019 with the total miles that a bus traveled 2017 and 2018. The average utilization per route shown in Table 3 is calculated as follows: for Route B, for instance, one takes the average of all buses that have an average number of bus stops per mile equal to that of Route B. For the system average, the average utilization is the average across all transit buses.

The two routes A and B yield extreme findings for the range of routes operated by Marguerite, because they entail the highest and lowest average fuel consumption per hour observed for diesel buses in the data set. Other routes of the system entail values in between, with the system average amounting to 4.44 gallons per hour. This can largely be attributed to the observation that more bus stops per mile reduce the average miles per hour traveled on a route. Route A exhibits one of the highest values for average velocity, while the opposite holds for Route B. In contrast to the relatively small energy cost of electric buses, the fuel cost for diesel buses becomes the dominant factor in determining the critical utilization rate and, by implication, the cost-minimizing composition of the bus fleet (see Figure 3).

Miles Traveled as the Output Measure. The application to transit buses in Section 4 focused on the output measure of passenger-miles for the transportation service in question.

Figure 4 shows the life-cycle cost curves for both electric and diesel buses on routes A and B as a function of miles, rather than passenger-miles, traveled. We refer to this cost curve as $LCM(\cdot)$. Since $b(\cdot|\theta) > 1$ for both routes, the generic expression for the levelized cost of X-miles shows that the $LCM(\cdot)$ curve decreases more steeply than the $LCPM(\cdot)$ curve for all values of h. Thus $|LCPM'(h)| < |LCM'(h)|$ for all h.

We recall from Figure 1 that the $LCPM$ for both types of drivetrains decreases as one switches from Route A to Route B. Yet, the opposite change is observed for $LCPM$ in Figure 4. This opposite movement reflects that there are on average 9.4 passengers who complete Route B, while there are only 3.2 such passengers on Route A. Comparison of Figure 1 and Figure 4 also illustrates that the critical utilization rate h^* is invariant to the measure of output. In general, we conclude that for any given drivetrain the magnitude and shape of the levelized cost curve depends on the specific measure of X-miles. However, both the life-cycle cost comparison across drivetrains, that is, the critical utilization rate h^*, and the cost minimizing composition of the vehicle fleet are unaffected by the actual measure of X-miles.

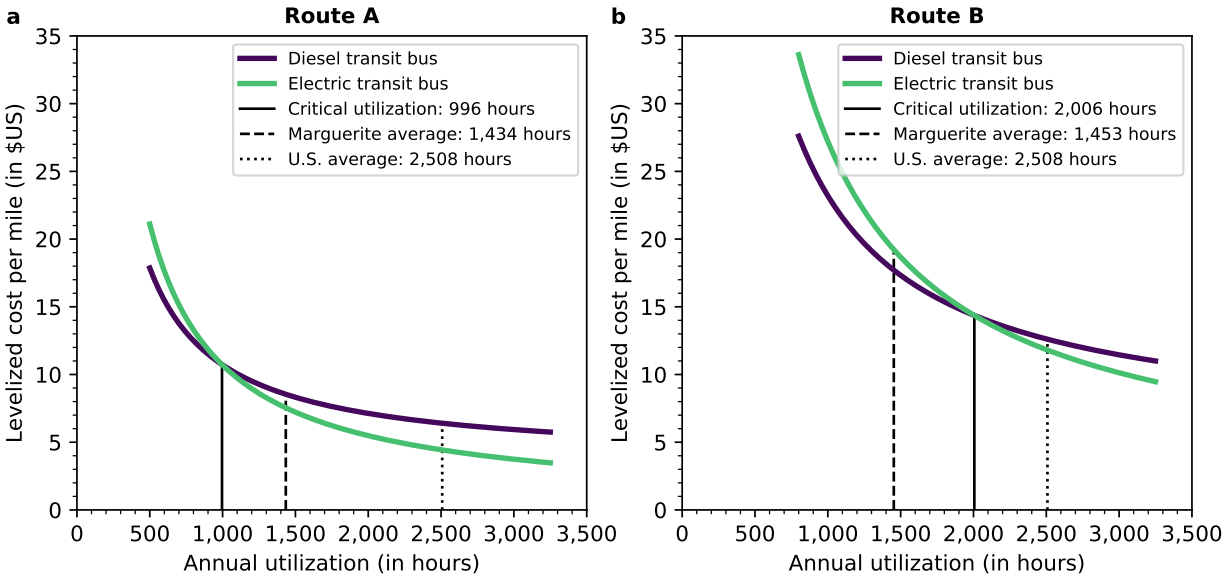


Figure 4: **Levelized cost per passenger-mile. a,b,** This figure shows the levelized cost per mile of diesel and electric transit buses for (**a**) Route A and (**b**) Route B.

8 Data availability

The data used in this study are referenced in the main body of the paper and the Supplementary Information. Additional data and information is available from the corresponding author upon reasonable request.

9 Acknowledgments

We received helpful suggestions from Amadeus Bach, Felix Baumgarte, Stefanie Burgahn, Veronika Grimm and colleagues at the University of Mannheim and Stanford University. The cost estimates reported in Section 4 were made available to us by the Department of Transportation at Stanford University. We thank Brian Shaw for supporting our data collection effort; we also express our particular appreciation to Brian Jackson for his continued willingness to guide us through the details of Stanford's bus operation. Finally, we acknowledge the excellent research assistance of Carlos Manuel Ciudad-Real.

10 Author contributions

The authors contributed equally to the conceptualization and development of the paper. S.R. lead the model development, S.C. lead the data collection, and G.G. lead the empirical analysis. All authors contributed substantively to the writing of the paper.

11 Competing interests

The authors declare no competing financial or non-financial interests.

References

[1] BNEF. Electric vehicle outlook 2019. Report, Bloomberg New Energy Finance, New York, NY (2019).

[2] IEA. *Global EV Outlook 2019* (2019). URL https://www.oecd-ilibrary.org/content/publication/35fb60bd-en.

[3] Arbib, J. & Seba, T. *Rethinking Transportation 2020-2030* (Rethink X, 2018).

[4] Needell, Z. A., McNerney, J., Chang, M. T. & Trancik, J. E. Potential for widespread electrification of personal vehicle travel in the united states. *Nature Energy* **1**, 16112 (2016). URL https://doi.org/10.1038/nenergy.2016.112.

[5] He, X. *et al.* Economic and climate benefits of electric vehicles in china, the united states, and germany. *Environmental Science & Technology* **53**, 11013–11022 (2019). URL https://doi.org/10.1021/acs.est.9b00531.

[6] Kamargianni, M., Li, W., Matyas, M. & Schäfer, A. A critical review of new mobility services for urban transport. *Transportation Research Procedia* **14**, 3294 – 3303 (2016). URL http://www.sciencedirect.com/science/article/pii/S2352146516302836. Transport Research Arena TRA2016.

[7] Matyas, M. & Kamargianni, M. The potential of mobility as a service bundles as a mobility management tool. *Transportation* **46**, 1951–1968 (2019). URL https://doi.org/10.1007/s11116-018-9913-4.

[8] Taiebat, M. & Xu, M. Synergies of four emerging technologies for accelerated adoption of electric vehicles: Shared mobility, wireless charging, vehicle-to-grid, and vehicle automation. *Journal of Cleaner Production* **230**, 794 – 797 (2019). URL http://www.sciencedirect.com/science/article/pii/S0959652619316683.

[9] Wadud, Z. Fully automated vehicles: A cost of ownership analysis to inform early adoption. *Transportation Research Part A: Policy and Practice* **101**, 163 – 176 (2017). URL http://www.sciencedirect.com/science/article/pii/S096585641630739X.

[10] Nurhadi, L., Borén, S., Ny, H. & Larsson, T. Competitiveness and sustainability effects of cars and their business models in swedish small town regions. *Journal of Cleaner Production* **140**, 333 – 348 (2017). URL http://www.sciencedirect.com/science/article/pii/S0959652616303134. Systematic Leadership towards Sustainability.

[11] Chen, X. *et al.* Impacts of fleet types and charging modes for electric vehicles on emissions under different penetrations of wind power. *Nature Energy* **3**, 413–421 (2018). URL https://doi.org/10.1038/s41560-018-0133-0.

[12] Knobloch, F. *et al.* Net emission reductions from electric cars and heat pumps in 59 world regions over time. *Nature Sustainability* (2020). URL https://doi.org/10.1038/s41893-020-0488-7.

[13] Lebeau, P., Macharis, C., Mierlo, J. & Lebeau, K. Electrifying light commercial vehicles for city logistics? a total cost of ownership analysis. *European Journal of Transport and Infrastructure Research* **15** (2015). URL https://superheroscitech.tudelft.nl/ejtir/article/view/3097.

[14] Lajunen, A. & Lipman, T. Lifecycle cost assessment and carbon dioxide emissions of diesel, natural gas, hybrid electric, fuel cell hybrid and electric transit buses. *Energy* **106**, 329 – 342 (2016). URL http://www.sciencedirect.com/science/article/pii/S036054421630319X.

[15] Tong, F., Hendrickson, C., Biehler, A., Jaramillo, P. & Seki, S. Life cycle ownership cost and environmental externality of alternative fuel options for transit buses. *Transportation Research Part D: Transport and Environment* **57**, 287 – 302 (2017). URL http://www.sciencedirect.com/science/article/pii/S136192091630476X.

[16] Durango-Cohen, P. L. & McKenzie, E. C. Trading off costs, environmental impact, and levels of service in the optimal design of transit bus fleets. *Transportation Research Procedia* **23**, 1025 – 1037 (2017). URL http://www.sciencedirect.com/science/article/pii/S235214651730337X. Papers Selected for the 22nd International Symposium on Transportation and Traffic Theory Chicago, Illinois, USA, 24-26 July, 2017.

[17] Islam, A. & Lownes, N. When to go electric? a parallel bus fleet replacement study. *Transportation Research Part D: Transport and Environment* **72**, 299 – 311 (2019). URL http://www.sciencedirect.com/science/article/pii/S1361920918309829.

[18] Xu, Y. *et al.* Assessment of alternative fuel and powertrain transit bus options using real-world operations data: Life-cycle fuel and emissions modeling. *Applied Energy* **154**, 143 – 159 (2015). URL http://www.sciencedirect.com/science/article/pii/S0306261915005759.

[19] Giordano, A., Fischbeck, P. & Matthews, H. S. Environmental and economic comparison of diesel and battery electric delivery vans to inform city logistics fleet replacement strategies. *Transportation Research Part D: Transport and Environment* **64**, 216 – 229 (2018). URL http://www.sciencedirect.com/science/article/pii/S1361920916308525. The contribution of electric vehicles to environmental challenges in transport. WCTRS conference in summer.

[20] Palmer, K., Tate, J. E., Wadud, Z. & Nellthorp, J. Total cost of ownership and market share for hybrid and electric vehicles in the UK, US and Japan. *Applied Energy* **209**, 108–119 (2018). URL https://doi.org/10.1016/j.apenergy.2017.10.089.

[21] APTA. 2019 public transportation fact book. Report 70th Edition, American Public Transportation Association, Washington DC (2019).

[22] Comello, S. & Reichelstein, S. The emergence of cost effective battery storage. *Nature Communications* **10**, 2038 (2019). URL http://www.nature.com/articles/s41467-019-09988-z.

[23] MIT. The Future of Coal: Options for a Carbon-Constrained World. Tech. Rep. ISBN 978-0-615-14092-6, Massachusetts Institute of Technology, Cambridge, MA (2007).

[24] Reichelstein, S. & Rohlfing-Bastian, A. Levelized Product Cost: Concept and Decision Relevance. *The Accounting Review* **90**, 1653–1682 (2015).

[25] Kaplan, R. S. & Anderson, S. R. *Time-driven activity-based costing: a simpler and more powerful path to higher profits* (Harvard business press, 2007).

[26] Glenk, G. & Reichelstein, S. Synergistic value in vertically integrated power-to-gas energy systems. *Production and Operations Management* **29**, 526–546 (2020). URL https://onlinelibrary.wiley.com/doi/abs/10.1111/poms.13116. https://onlinelibrary.wiley.com/doi/pdf/10.1111/poms.13116.

[27] CARB. Hybrid and Zero-Emission Truck and Bus Voucher Incentive Project (2020). URL https://www.californiahvip.org/how-to-participate/#Eligible-Vehicle-Catalog.

[28] Schmidt, O., Hawkes, A., Gambhir, A. & Staffell, I. The future cost of electrical energy storage based on experience rates. *Nature Energy* **6**, 17110 (2017).

[29] Schmidt, O., Melchior, S., Hawkes, A. & Staffell, I. Projecting the future levelized cost of electricity storage technologies. *Joule* **3**, 81 – 100 (2019). URL http://www.sciencedirect.com/science/article/pii/S254243511830583X.

[30] Jiao, N. & Evans, S. *Business Models for Repurposing a Second-Life for Retired Electric Vehicle Batteries*, 323–344 (Springer International Publishing, Cham, 2018). URL https://doi.org/10.1007/978-3-319-69950-9_13.

[31] Martinez-Laserna, E. *et al.* Battery second life: Hype, hope or reality? a critical review of the state of the art. *Renewable and Sustainable Energy Reviews* **93**, 701 – 718 (2018). URL http://www.sciencedirect.com/science/article/pii/S1364032118302491.

[32] Glenk, G. & Reichelstein, S. Economics of Converting Renewable Power to Hydrogen. *Nature Energy* **4**, 216–222 (2019).

[33] Stanford University. Historical Utilities Rates - Charge Out Rates (2020). URL https://lbre.stanford.edu/sem/historical-utilities-rates.

[34] de Chalendar, J. A., Glynn, P. W. & Benson, S. M. City-scale decarbonization experiments with integrated energy systems. *Energy Environ. Sci.* **12**, 1695–1707 (2019). URL `http://dx.doi.org/10.1039/C8EE03706J`.

[35] Eudy, L., Prohaska, R., Kelly, K. & Post, M. Foothill transit battery electric bus demonstration results. Report NREL/TP-5400-65274, National Renewable Energy Laboratory, Golden, CO (2016).

[36] Elgqvist, E. M. Economics of solar pv and stationary storage for electric bus charging in missoula, montana .

Supplementary Information

Supplementary Table 1: **List of Symbols and Acronyms.**

Variable	Unit	Description
α	%	Corporate income tax rate
Δ	–	Tax factor
γ	–	Discount factor
λ	%	Share of acquisition expenditure yielding the salvage value
θ	–	Description of duty cycle
$a(\theta)$	miles/hour	Average velocity
$b_i(h\|\theta)$	passengers or tons	Number of passengers or mass transported in year i
BMS	–	Battery management system
$c(h\|\theta)$	\$/X-mile	Levelized acquisition cost
CFL_i^o	\$	Annual pre-tax cash flow in year i
d_t	–	Depreciation Schedule
$D(k)$	hours	Total time during which at least k vehicles must be in operation
$f(h\|\theta)$	\$/X-mile	Levelized fixed cost
$F_i(\theta$	\$/year	Fixed operating cost in year i
$H(k_i)$	hours	Number of daily operating hours of a drivetrain i
h_i	hours	Hours of operation in year i
$\overrightarrow{h}$	hours	Usage profile
I_i	\$/year	Taxable income in year i
k	–	Number of vehicles
$L(t)$	in k	Load profile per hour t
LCM	\$/mile	Levelized cost per mile
$LCOE$	\$/kWh	Levelized cost of electricity
$LCPM$	\$/passenger-mile	Levelized cost per passenger-mile
$LCXM$	\$/X-mile	Levelized cost per X-mile
kWh	–	Kilowatt hour
p	\$/X-mile	Revenue attained per X-mile
r	%	Interest rate
T	years	Useful lifetime of a given vehicle
TCO	\$	Total cost of ownership
v	\$	Acquisition expenditure of the transportation vehicle
$w_i(h\|\theta)$	\$/year	Variable operating cost in year i
$w(h\|\theta)$	\$/X-mile	Levelized variable operating cost
$X_i(\overrightarrow{h}\|\theta)$	X-mile	Output measure, where X depends on $b_i(h\|\theta)$ in year i
$Y(\overrightarrow{h}\|\theta)$	X-miles	Levelization factor

Supplementary Table 2: **General Specifications for the Examined Buses.**

Specification	**Diesel**	**Electric**
Make	Gillig MA	BYD K9 Electric Bus
Vintage (year & number in fleet)	2003 (8)	2013 (1), 2014 (10), 2017 (18)
Gross Vehicle Weight [lbs]	39,600	40,786
Length [ft]	35	35.8
Passenger Capacity	32	34
Drivetrain	Cummins ISB 5.9L I6; 235hp; 460 lb-ft torque	AC synchronous motor; 80 kW, 350 kWh iron-phosphate battery

Supplementary Note 1. Transit Bus System Route Data.

Route data for the Stanford Marguerite transit bus system examined in Section 4 of the manuscript, including system map and bus stop locations is found at the Stanford Transportation website:

`https://transportation.stanford.edu/marguerite/view-maps-and-schedule`.

Route information, including the number of bus stops per mile, the average velocity, average number of passengers per hour, and the average number of passenger-miles per passenger is provided in Supplementary Table 3. Note that actual route names found on the Stanford Transportation site have been anonymized in an effort to maintain a basic level of data security and privacy.

Supplementary Table 3: **Stanford Transportation Transit Bus System Route Data.**

Route	Stops/mile	Velocity [mph]	Passenger/hour	Passenger-mile/passenger
A	1.1	7.4	23	1.0
B	2.7	3.0	40	0.7
C	1.4	8.5	19	1.2
D	0.8	21.2	20	2.5
E	1.2	10.8	22	1.5
F	1.2	8.9	14	3
G	1.7	7.2	55	1.1
H	2.0	7.9	24	2.5
I	2.5	10.9	50	1.2
J	2.7	8.2	103	1
K	1.7	6.5	38	1.2
L	1.7	7.9	24	2.8
M	2.5	8.0	81	1.2
N	2.0	8.0	31	1.2
O	2.7	8.2	15	1.2

Supplementary Note 2. Constituent Variable and Fixed Costs

Stanford Transportation provided detailed operational cost data. Variable operating and fixed operating costs, as defined in Section 2 of the manuscript, are aggregations of cost subcategories provided in Supplementary Table 4. For each cost subcategory listed, its applicability is indicated per drivetrain, as well as to which operational cost, variable or fixed, it belongs. The allocation of subcategory costs to either variable or fixed was verified with respective experts at Stanford Transportation.

Supplementary Table 4: **Variable and Fixed Cost Categories per Drivetrain.**

Cost category	**Diesel**	**Electric**	**Cost type**
HVAC	yes	yes	fixed
Air Intake System	yes	no	fixed
Brakes	yes	yes	variable
Cab-Sheet Metal	yes	yes	fixed
Charging System	yes	yes	fixed
Clean-up/ Detailing	yes	yes	fixed
Cooling System	yes	yes	variable
Cranking System	yes	yes	variable
Diesel Exhaust Fluid	yes	no	variable
Tires	yes	yes	variable
Dry Freight Body	yes	yes	fixed
Electric Prop. System	no	yes	variable
Electrical Access.	yes	yes	fixed
Exhaust System	yes	no	variable
Expendables	yes	yes	variable
Frame	yes	yes	fixed
Front Axle-Susp-Brgs	yes	yes	variable
Fuel System	yes	no	variable
General Accessories	yes	yes	variable
Horn-mounting	yes	yes	fixed
Ignition System	yes	no	fixed
Instruments	yes	yes	fixed
Liftgate	yes	yes	fixed
Lighting System	yes	yes	fixed
Lines	yes	yes	fixed
Main Auto Trans	yes	no	variable
Mounted Equip Repair	yes	yes	fixed
Oil	yes	no	variable
Power Plant	yes	yes	fixed
Radio	yes	yes	fixed
Rear Axle-Susp-Brgs	yes	yes	variable
Rear Door	yes	yes	fixed
Refrig-Mechanical	yes	yes	variable
Satellite/Veh Comm	yes	yes	fixed
Special	yes	yes	fixed
Steering	yes	yes	variable
Suppl Info Devices	yes	yes	fixed
Towing	yes	yes	variable
Trim	yes	yes	fixed
Valves	yes	yes	variable
Wash	yes	no	fixed
Wheels-Rims-Hubs	yes	yes	variable